MR Myocardial Perfusion Imaging[1]

Otavio R. Coelho-Filho, MD, MPH
Carsten Rickers, MD
Raymond Y. Kwong, MD, MPH
Michael Jerosch-Herold, PhD

Contrast material–enhanced myocardial perfusion imaging by using cardiac magnetic resonance (MR) imaging has, during the past decade, evolved into an accurate technique for diagnosing coronary artery disease, with excellent prognostic value. Advantages such as high spatial resolution; absence of ionizing radiation; and the ease of routine integration with an assessment of viability, wall motion, and cardiac anatomy are readily recognized. The need for training and technical expertise and the regulatory hurdles, which might prevent vendors from marketing cardiac MR perfusion imaging, may have hampered its progress. The current review considers both the technical developments and the clinical experience with cardiac MR perfusion imaging, which hopefully demonstrates that it has long passed the stage of a research technique. In fact, cardiac MR perfusion imaging is moving beyond traditional indications such as diagnosis of coronary disease to novel applications such as in congenital heart disease, where the imperatives of avoidance of ionizing radiation and achievement of high spatial resolution are of high priority. More wide use of cardiac MR perfusion imaging, and novel applications thereof, are aided by the progress in parallel imaging, high-field-strength cardiac MR imaging, and other technical advances discussed in this review.

©RSNA, 2013

A survey of the National Library of Medicine's PubMed database with the keywords "myocardial perfusion" and "magnetic resonance" reveals a steadily increasing number of publications during the past decade, which points toward progress of the field but still amounts to less than 30% of publications, if studies based on nuclear imaging, such as single photon emission computed tomography (SPECT) and positron emission tomography (PET), are included in the search. This dynamic growth has also led to a plethora of techniques and approaches for assessing myocardial perfusion with magnetic resonance (MR) imaging. The field continues to advance rapidly due to the introduction of new approaches for accelerating MR image acquisition, improving signal-to-noise ratio (SNR) and contrast-to-noise ratio, and migrating to higher magnetic field strengths. The purpose of this review is to summarize the current state of myocardial perfusion imaging with use of cardiac MR, including recent technical advancements, and the published evidence pointing to its clinical benefits.

Essentials

- Dynamic contrast-enhanced MR imaging of the heart, at rest and during stress, is a diagnostic and prognostic tool to guide therapy in the clinical setting.
- Myocardial perfusion MR imaging is not inferior to gated single photon emission computed tomography for the diagnosis of coronary artery disease (CAD).
- T1-weighted, cardiac-gated, single-shot, two-dimensional, and multisection acquisitions are currently the preferred approach to depict myocardial contrast-enhancement for CAD diagnosis.
- Parallel imaging acceleration and sparse temporal sampling are essential for whole-heart coverage and may allow full three-dimensional acquisitions in the future.

Coronary Physiology at Rest and during Hyperemia

The established physiologic rationale for stress perfusion imaging rests on the concept of coronary flow reserve (1). Coronary flow reserve refers to the capacity of the coronary circulation to increase blood flow through the coronary tree, when the perfusion bed is maximally dilated. In a clinical cardiac MR examination, coronary vasodilation is typically achieved with a pharmacological agent such as adenosine. Although other mechanisms such adrenergic stimulation, for example, through the cold pressor test, also result in some vasodilation and flow increase (2), adenosine receptor agonists such as adenosine cause, in healthy adult subjects, an up to four-fold increase of coronary flow and are particularly effective in minimizing the resistance of the distal coronary perfusion bed. Lowering of the distal coronary resistance can reveal the presence of flow-limiting lesions in the epicardial arteries. At rest, an epicardial lesion will become flow limiting only with a luminal narrowing of approximately 85% or higher, while with maximal vasodilation, this threshold is lowered to approximately 50% or higher (3,4). The coronary flow response during vigorous exercise will be of the same magnitude as the increase observed during maximal vasodilation with an agent such as intravenous adenosine (5).

The determination of the coronary flow reserve entails a measurement of resting coronary flow and a second measurement during maximal vasodilation. Typically, a flow (or velocity) ratio is formed to quantify the coronary flow reserve (eg, through cine phase-contrast MR imaging, or invasively, with a Doppler wire). Flow and velocity can be used here interchangeably because flow represents the product of flow velocity times the lumen area (or the integral of velocity over the lumen area). In this review, we will describe cardiac MR methods for measuring a closely related quantity, the myocardial perfusion reserve. Perfusion refers here to the blood flow through the coronary

microcirculation, meaning the volume of blood flowing through a volume, or mass unit of myocardium, per unit of time. Assuming that myocardial perfusion can be quantified independently at rest and during maximal vasodilation, one can calculate the myocardial perfusion reserve, analogous to the coronary flow reserve, as the ratio of hyperemic flow divided by the resting flow. In a healthy coronary circulation, the coronary flow reserve and the myocardial perfusion reserve agree in magnitude, but with epicardial disease, the presence of coronary collaterals can result in an epicardial flow reserve, which is lower than the myocardial perfusion reserve measured downstream from the lesion (6). The myocardial perfusion reserve, rather than the coronary flow reserve, is, arguably, a closer and potentially more accurate measure of the capacity of the coronary circulation to deliver sufficient oxygen to a given region of interest in the heart muscle. An impaired myocardial perfusion reserve is therefore considered a useful surrogate marker for ischemia, although the threshold below which the myocardial perfusion reserve needs to decrease to cause clinically significant ischemia is not well defined. A coronary flow reserve threshold (2.5:1 in reference 7) has been used as cut-off, as it results in a significant association with risk factors, presence of coronary artery disease (CAD), or with patient outcomes after revascularization (7).

Principles of Myocardial Perfusion Imaging with Cardiac MR

The coronary flow reserve can be measured with cardiac MR imaging by means of direct visualization of the

lumen of the proximal coronary artery and with quantification of blood flow velocity in the vessel lumen by using the phase-contrast technique (8). This remains a challenging type of examination due to cardiac and respiratory motion and the relatively small lumen dimensions (approximately 1.5–3 mm). Flow through the coronary microcirculation can only be assessed indirectly, either by labeling the blood and observing signal intensity changes resulting from the transit of the labeled blood or by introducing a blood-borne MR-detectable tracer and observing the injected tracer through the myocardium. The measurement of contrast enhancement during the first pass of a contrast agent bolus through the cardiac chambers and the myocardium is currently the most widely used and reliable technique to assess myocardial perfusion. It is often referred to as first-pass imaging. Cardiac perfusion studies with MR rely primarily on the use of T1-weighted techniques, while for brain perfusion it is more common to use T2*-weighted techniques. The reason lies in the difference in the distribution of the volume of gadolinium chelates, which normally cannot cross the blood-brain barrier, and the higher vascular volume in the heart compared with the brain. To track the first pass of a contrast agent bolus through the cardiac chambers and myocardium, while freezing cardiac motion, one applies dynamic imaging techniques that allow acquisition of an image during a fraction of a heartbeat, which is repeated every heartbeat during the first pass and ideally covers a stack of sections through the heart. Figure 1 is a conceptual illustration of the principle of contrast material–enhanced, first-pass perfusion imaging.

An alternative approach is based on labeling blood as an endogenous tracer by applying a spatially selective inversion preparation and tracking the signal changes that result from the flow of the inverted spins in or out of an adjacent region (9). This method has given rise to a slew of techniques, referred to as arterial spin labeling, but their use in the heart remains limited and almost absent in clinical settings because of confounding effects of cardiac motion and the relative modest signal changes achievable with spin labeling (10,11).

Cardiac MR Pulse Sequence Techniques

A survey of pulse sequence techniques that are used for contrast-enhanced myocardial perfusion imaging (first-pass imaging) could start off with an identification of its key components. They are T1 contrast enhancement characteristics and image readout, with image readout defined as the ensemble of radiofrequency excitations and gradient pulses for image encoding performed for acquisition of an image. With most pulse sequence techniques for first-pass imaging, these two aspects are dealt with by first applying a magnetization preparation for T1 weighting followed by image readout. The magnetization preparation can be a saturation preparation (12), which by definition nulls the bulk longitudinal and dephases the transverse magnetization components, or an inversion preparation. The image readout, mostly in the form of sequential two-dimensional acquisitions for multiple sections, follows magnetization preparation, with a possible delay that controls the T1 weighting of the measured signal. For the image readout, the primary concerns are the time it takes to read out the image, the SNR, a lack of motion artifacts or susceptibility artifacts, and a need to preserve the T1 weighting introduced by the magnetization preparation that precedes the image readout. Although motion artifacts can be reduced already by virtue of fast image readout, the readout of the signal can, even with very fast image readout, be corrupted by motion if one uses a long echo time. Therefore, one of the fastest image acquisition methods, the echo-planar technique (13), is seldom used in its "unsegmented" form for myocardial perfusion imaging, but rather in a hybrid form, with echo-train lengths typically of five to six echoes or fewer after each radiofrequency pulse (14). Also the transit of a contrast agent bolus through the ventricular cavities can cause susceptibility artifacts (in particular at higher field strength) (15) and a shift of the proton resonance frequency (16) in adjacent regions, which suggests that techniques sensitive to magnetic susceptibility effects and/or frequency shifts (eg, steady-state free precession imaging) should be avoided. For any quantitative analysis of myocardial perfusion, special consideration must be given to the contrast enhancement in the blood pool. The arterial contrast enhancement should be sampled without too much saturation, that is, the contrast enhancement should be in approximately linear relation to the concentration of a contrast agent in the blood. To address this requirement, the "dual bolus" (17) and "dual contrast" were introduced (18). Table 1 summarizes the sequence techniques that are most commonly used for myocardial perfusion imaging.

Figure 2 illustrates the cardiac MR stress protocol that we are currently using at our institution. In a myocardial perfusion study, the images are acquired during approximately 60 heartbeats to cover a precontrast phase, the first pass of the contrast agent after its injection, and the recirculation of contrast agent. The total acquisition time is too long for a single breath hold, although patients are typically asked to hold their breath for the initial phase of the study and resume breathing when necessary, without having to take a deep breath. Breathing motion is sufficiently slow that it does not cause motion artifacts, but during postprocessing it becomes necessary to correct for cardiac motion, and through-plane motion causes section misregistration. As an alternative, section-tracking techniques have been developed that use a navigator pulse to track diaphragmatic motion and dynamically adjust the section positions so that the same anatomic region is tracked during the entire perfusion imaging (19,20). It may well be that automatic image postprocessing techniques prove more effective in coping with the correction for in-plane breathing motion (21), but full-motion correction by postprocessing (including through-plane motion) would

Radiology
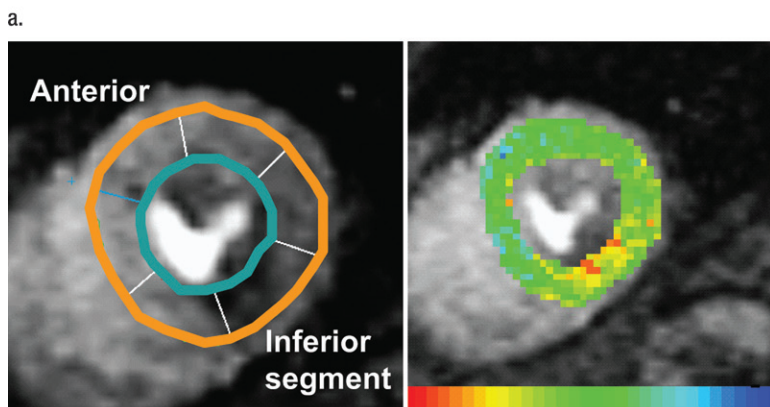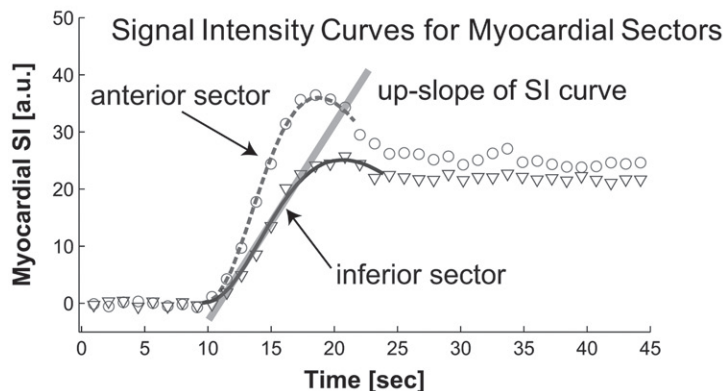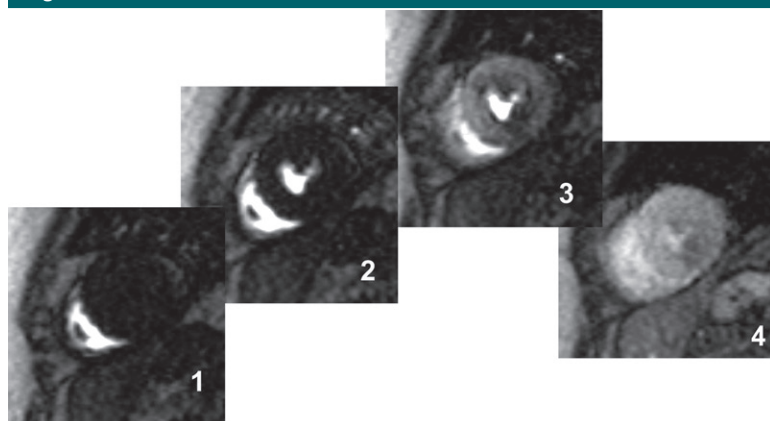
Figure 1

Figure 1: **(a)** Frames *1–4* acquired during adenosine-induced hyperemia in a 64-year-old woman with CAD as part of first-pass perfusion study with a saturation-recovery-prepared gradient-echo sequence covering four sections during each heartbeat. A 0.05 mmol/kg bolus of gadolinium-based contrast agent was injected during approximately three heartbeats after the start of image acquisition by using a power injector (4 mL/sec injection rate). The graph shows signal intensity *(SI)* changes in anterior and inferior myocardial sectors, with the latter showing reduced myocardial enhancement. The linear rate of contrast enhancement (up-slope) is a parameter sensitive to myocardial blood flow differences. *a.u.* = arbitrary units. **(b)** For postprocessing, the perfusion MR images are segmented (left) along endo- and epicardial borders (solid contours). The left ventricular wall is subdivided into six segments, using the anterior left ventricular-right ventricular junction as reference point. Signal intensity curves are generated for each pixel location. Pixel locations were tracked over all images by their transmural (distance between endo- and epicardial contours) and circumferential (angle from reference point) coordinates. The parametric map (right) shows the spatial variation of the color-encoded up-slope parameter.

is based on acquisition of a subset of spatial-encoding steps for every image, with the encoding steps typically clustered around low spatial frequencies (low k-space), as they provide a low resolution approximation to the target image. Higher spatial frequencies are sampled or updated less frequently. This type of technique was initially introduced under the label of "keyhole" technique (23). Arguably, it never found much acceptance for myocardial perfusion imaging, but it paved the way, in combination with parallel imaging techniques, for more advanced methods, such as k-space and time (k-t) broad-use linear acquisition speed-up technique (BLAST) (24,25) and k-t generalized autocalibrating partially parallel acquisition (GRAPPA) (26–28). These technical developments for imaging acceleration are available on all new imagers with dedicated cardiac MR application packages and phased-array coils for cardiac imaging, though myocardial perfusion imaging with cardiac MR was feasible and used without access to parallel imaging techniques, albeit with heart coverage limited to two to three sections per heartbeat.

probably require three-dimensional (3D) acquisitions rather than multisection imaging.

Imaging Acceleration and Sparse Sampling

Image acceleration techniques have had a strong, positive impact on cardiac perfusion imaging and allowed improvement in section coverage or temporal resolution (22). These developments started out with parallel imaging techniques, which take advantage of variations in the spatial sensitivity profiles of coil elements in a phased array to reduce the number of spatial phase-encoding steps.

Another type of acceleration technique, long known in MR imaging,

SNR and contrast-to-noise ratio are one of the limiting factors for speed-ups

Radiology

Table 1

Myocardial Perfusion Sequence Techniques and Parameters

Technique Acronyms	Description	Typical Parameters and Advantages	Image Acquisition Time/Parallel Imaging Acceleration Factor	Limitation
Turbo FLASH, turbo fast field echo, GRASS	GRE image acquisition with short TR and TE and magnetization preparation (saturation or inversion)	TR/TE msec, 3/1; 15° flip angle; 2D multisection; 8–10-mm sections; bandwidth, 600–800 Hz per pixel; nonsection-selective SR; relative immune against off-resonance and susceptibility effects	150–200 msec per section/two	Image acquisition speed slower than SSFP and hybrid EPI-GRE; low CNR and SNR compared with SSFP
Turbo SSFP, turbo balanced field echo, turbo FIESTA	SSFP acquisition with magnetization preparation (saturation or inversion)	2/1/; 40° flip angle; 2D multisection; 8-mm sections; bandwidth, 1000–12 000 Hz per pixel; SR; high CNR	130–160 msec per section/two to three	Off-resonance artifacts; bolus-induced frequency shifts; not suitable for > 1.5 T
Hybrid EPI-GRE	2D multisection, hybrid EPI-GRE acquisition with echo-train length of less than 6 and magnetization preparation	8/3; 15° flip angle; 8–10-mm sections; bandwidth, 600–800 Hz per pixel; shortest image acquisition time	100–150 msec per section/two	Susceptibility artifacts with long echo trains; echo-train length less than approximately 3 for 3 T

Note.—CNR = contrast-to-noise ratio, EPI = echo-planar imaging, FLASH = fast low-angle shot, GRASS = gradient refocused acquisition in steady state, GRE = gradient echo, SR = saturation preparation, SSFP = steady-state free precession, TE = echo time, TR = repetition time, 2D = two-dimensional.

in image acquisition, including the use of parallel imaging techniques, which involve trading off shorter acquisition times against a decrease in SNR (29). Performance of cardiac perfusion MR imaging at higher field strengths improves SNR, but at 3 T the choice of perfusion imaging techniques becomes more limited, as susceptibility and off-resonance artifacts grow more severe with increasing field strength. The demands on magnetization preparation methods also become more taxing (30). A study in 61 patients found that 3-T cardiac MR perfusion imaging is superior to imaging at 1.5 T for prediction of significant single- and multivessel coronary disease (29).

Future Technical Directions

Though 3D image acquisitions offer better SNR and can potentially achieve complete coverage of the heart without section misregistration, they are still seldom used for cardiac perfusion imaging due to some inherent limitations in preventing blurring and artifacts from cardiac motion. With a two-dimensional, multisection technique, images are acquired during different phases of the cardiac cycle, but the acquisition of each two-dimensional

image only takes a fraction of a heartbeat (~100–200 msec), and therefore cardiac motion is effectively frozen. For the 3D technique, encoding in the section direction is no longer spatially localized, and therefore motion during the entire 3D acquisition is reflected in the reconstructed sections. The constraint to acquire all data for a selected slab in a 3D acquisition in a fraction of a heartbeat is therefore not that different from a two-dimensional acquisition, but the total number of encoding steps is an order of magnitude larger. To overcome this limitation, for 3D cardiac perfusion imaging it will therefore require higher image acceleration, on the order of approximately 10 or higher (31). Such high image acceleration factors currently represent a substantial challenge and are an impediment to the use of 3D techniques for cardiac perfusion imaging.

Within the past couple of years, a surprising development was initiated by the theory of compressed sensing, developed by Candes and Wakin (32) and Lusting et al (33). For decades, the Nyquist theorem formed one of the pillars of signal-processing theory, until it was realized that for band-limited signals, one could sample at a rate lower than prescribed by the Nyquist theorem if

the signal had a sparse representation. A familiar example for a sparse representation is the JPEG (Joint Photographic Experts Group) image-encoding method, which can result in 80%–90% reduction in data size without causing appreciable image degradation. Compressive sampling is, loosely speaking, a generalization: Random subsets of the signal or image data are acquired in a sampling space (eg, k-space in the case of MR imaging), with some a priori assumptions about how the images could be given a sparse representation with a particular type of encoding. Compressive sensing carries considerable promise for further acceleration of myocardial perfusion imaging (34) and can be combined with parallel imaging acceleration for further gains.

Another promising technique is highly constrained back-projection reconstruction, or HYPR (35), which involves acquisition of a highly reduced (eg, by factor of four or higher) subset of radial projections during each cardiac cycle so that a full set of radial projections is updated at a much slower rate (eg, over four cardiac cycles). A composite image is constructed from the full set of radial projections and used to constrain the reconstruction of images for each cardiac cycle from
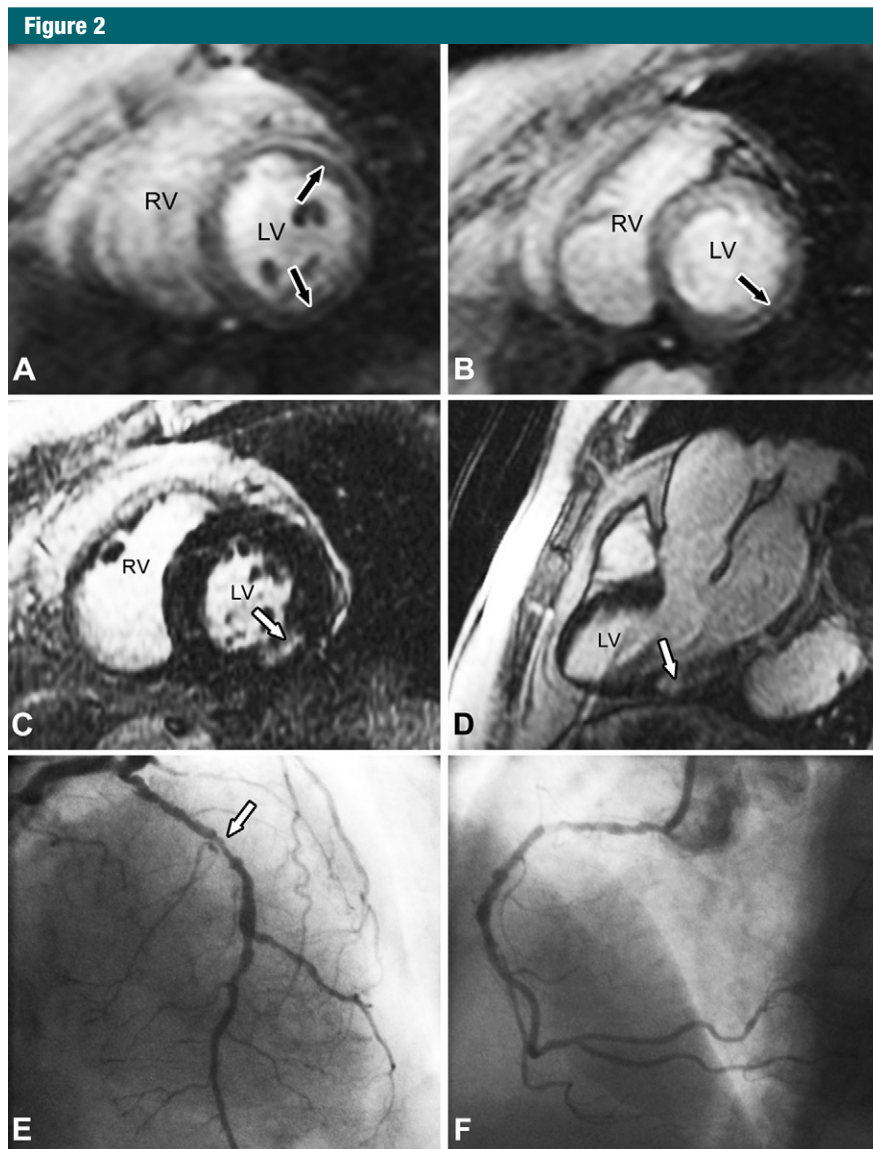
Figure 2

Figure 2: Stress MR myocardial perfusion study in 67-year-old woman with exertional chest pain who was referred for ischemia assessment. *A,* Stress and, *B,* rest first-pass perfusion images show ischemia in anterolateral wall and a fixed defect in the inferolateral walls (no stenosis) (arrows). *C, D,* Late gadolinium enhancement images show a nearly transmural myocardial infarction in the inferolateral wall (arrow) and viable myocardium everywhere else. *E, F,* Subsequent coronary angiograms ordered at the discretion of the referring physician show, *E,* critical luminal narrowing (arrow, >70%) in left anterior descending coronary artery and, *F,* no critical stenosis in the right coronary artery. *LV* = left ventricle, *RV* = right ventricle.

the highly reduced subsets of radial projections. HYPR has been applied successfully for myocardial perfusion studies, and the images were shown to have better SNR and better spatial resolution than conventional myocardial perfusion images (36,37).

Contrast Agents and Their Administration for Cardiac Perfusion Studies

Gadolinium chelates such as gadopentetate dimeglumine, which can distribute within the extracellular space of myocardial tissue, are the most widely used agents for cardiac perfusion studies. Intravascular agents have been used in experimental studies, but almost never in patient studies. There is some evidence from animal studies that the conspicuity of a perfusion defect can be observed longer with an intravascular contrast agent (38). This may reflect the reduced perfused vascular volume distal to a coronary stenosis.

When an injected tracer is used to demonstrate a blood flow deficit due to a flow-limiting epicardial lesion or microvascular dysfunction, it is paramount to inject the tracer sufficiently fast so that the injection is not the rate-limiting step for myocardial contrast enhancement. This entails the use of a contrast agent with peripheral venous injection rates of 3–4 mL/sec, in particular during pharmacological stress, when myocardial contrast enhancement is most likely to be constrained by the rate of contrast material injection.

Postprocessing and Quantification of Myocardial Perfusion

The clinically predominant mode of reading and interpreting myocardial perfusion studies is based on the visual interpretation of myocardial contrast enhancement when the perfusion images are displayed in cine mode. Regions with perfusion defects are characterized by a reduced rate of contrast enhancement. During early myocardial contrast enhancement such regions can be identified in cine frames by appearing hypointense. Playing the images in cine mode is essential for differentiating between image artifacts (in particular, so called dark-rim artifacts at the endocardial border) and true perfusion defects (39). A key distinguishing feature between dark-rim artifacts and true perfusion defects is the number of frames during which the signal hypointensity can be observed, with artifacts typically only appearing in a couple of frames during peak contrast enhancement in the blood pool and before peak contrast enhancement in the myocardial tissue. It has been shown that the prominence of such

Figure 3

Cardiac Localization	Stress Myocardial Perfusion Imaging	Ventricular Function	Rest Myocardial Perfusion Imaging	Ventricular Function	Late gadolinium enhancement
	Gd-DTPA (0.03-0.1 mmol/Kg) Bolus injection at 3-5ml/s	Cine SSFP	Gd-DTPA (0.03-0.1 mmol/Kg) Bolus injection at 3-5ml/s	Cine SSFP	Inversion recovery
	3-4 short-axis/per RR interval 60 RR intervals	10-12 short-axis (covering left ventricle)	3-4 short-axis/per RR interval 60 RR intervals	3 long-axis	10-12 short-axis (covering left ventricle)
					3 long-axis
	During infusion of vasodilator stress		During rest		
~3 minutes	~5 minutes	~12-15 minutes	~3 minutes	~2 minutes	~10-15 minutes
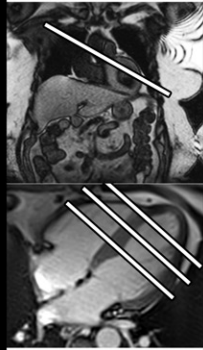
Figure 3: Illustration of the sequence of protocol components in a cardiac MR examination, which includes assessment of myocardial perfusion at rest and during vasodilator stress. The stress perfusion examination is generally performed before rest perfusion imaging to minimize a confounding effect of late gadolinium enhancement on the diagnostically most valuable part of the perfusion examination (vasodilator perfusion). This protocol is for single-bolus perfusion examinations, that is, without a small mini-bolus for arterial input assessment. *Gd-DTPA* = gadopentetate dimeglumine, *SSFP* = steady-state free precession.

artifacts can be reduced by increasing the spatial resolution in the phase-encoding direction (ie, increasing the number of phase-encoding steps), as this minimizes a well-known artifact from Fourier reconstruction (Gibbs artifact), which is thought to play an important role in the appearance of the dark-rim artifact (39).

A quantitative analysis of the myocardial perfusion is based on deriving parameter values from a time series of regional signal intensity values. The regions for such an analysis can be based on the definition of myocardial sectors (eg, standardized 17-segment model) or represent myocardial pixels to derive maps of myocardial perfusion with a spatial resolution equivalent to the underlying spatial resolution of the images (40–42). Both the sector- and pixel-based analyses require that the endo- and epicardial borders of the left ventricular wall be detected or traced for each image frame of a perfusion study, a task that still relies, to a large degree, on user intervention and represents the most time-consuming step of a quantitative analysis. Once this has been accomplished, the subsequent analysis

algorithms can be derived mostly without any further user intervention, parameters that relate to the rate of contrast enhancement, or the relative or absolute myocardial blood flow. The details of such an analysis are beyond the scope of this review and can be found in various references (17,43–47).

Myocardial Perfusion Imaging for Diagnosis of CAD

A substantial number of single-center (13,30,48,49) and multicenter (50,51) studies have confirmed the excellent sensitivity and specificity of myocardial perfusion imaging with vasodilator stress for the detection of CAD. These findings have been translated into steadily increasing clinical applications. Stress myocardial perfusion is a feasible, useful, and efficient tool for routine CAD diagnosis, with an example shown in Figures 3 and 4. In a multicenter study, Schwitter et al (52), using multivendor imagers and five different doses of gadopentetate dimeglumine, compared the diagnostic performance of stress myocardial perfusion cardiac MR with that of nuclear scintigraphy

in detecting significant CAD. They reported that 0.1 mmol/kg of gadopentetate dimeglumine yielded the highest accuracy in depicting CAD, defined as greater than 50% luminal narrowing in at least one vessel. On the basis of the receiver operating characteristic (ROC) analysis, Schwitter et al proved the noninferiority of stress myocardial perfusion cardiac MR to gated SPECT for CAD diagnosis (area under the ROC curve [AUC], 0.89 ± 0.06 vs 0.70 ± 0.06; $P < .05$). However, for multivessel CAD or if ungated SPECT studies were included, myocardial perfusion cardiac MR performed better than SPECT (multivessel disease: AUC, 0.89 ± 0.06 vs 0.70 ± 0.06, $P < .05$; at least one vessel disease: AUC, 0.86 ± 0.06 vs 0.67 ± 0.06; $P < .05$). Two recent meta-analyses (53,54) have confirmed the excellent diagnostic performance of stress myocardial perfusion cardiac MR in detection of significant CAD. Hamon and colleagues (54) combined data from more than 11 000 patients in 26 different studies to demonstrate an overall patient-based sensitivity of 0.89 (95% confidence interval [CI]: 0.88, 0.91) and specificity of 0.80 (95%
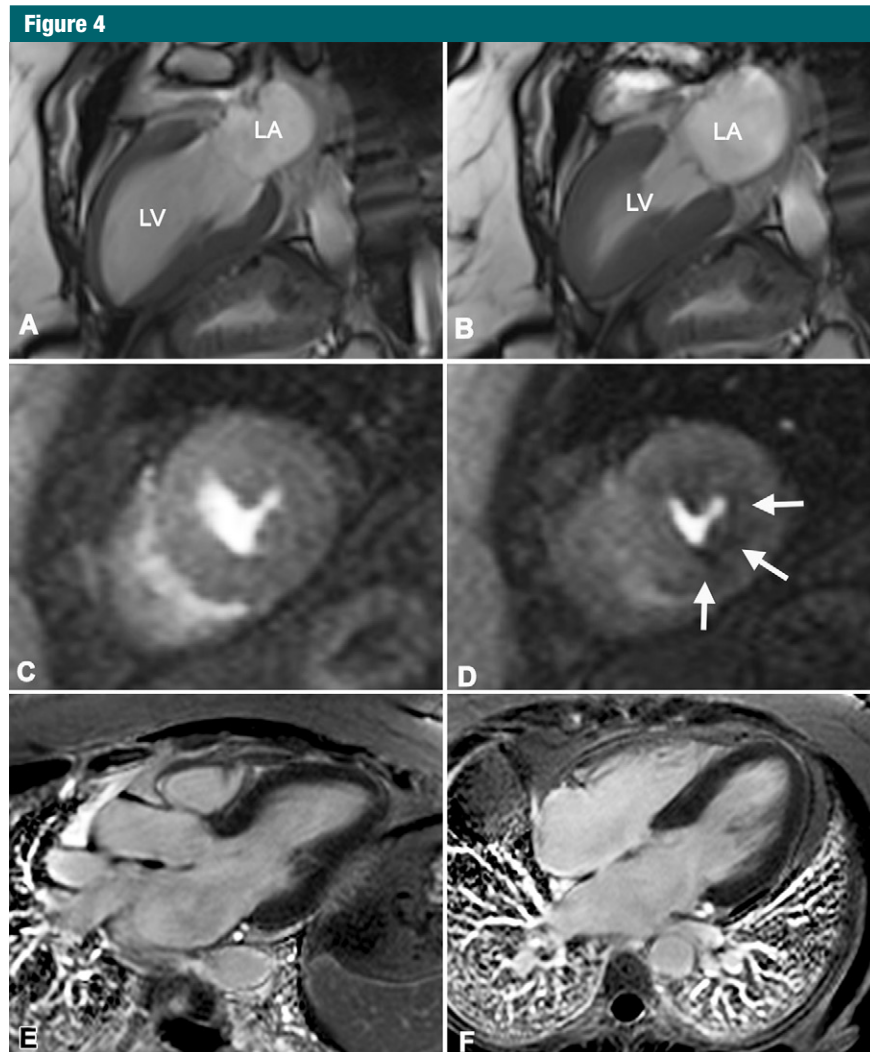
Figure 4: Vasodilator stress myocardial perfusion cardiac MR imaging in 49-year-old woman with hypertension and atypical chest pain. Coronary angiograpy performed after MR imaging revealed 90% right coronary artery lesion, which received a stent. Two-chamber cine steady-state free precession images at diastole *(A)* and systole *(B)* show normal resting function. First-pass gadolinium perfusion images during rest *(C)* and vasodilator stress *(D)* show a perfusion defect involving the middle to distal inferior and midinferolateral walls (arrows). Three-chamber *(E)* and four-chamber *(F)* late gadolinium enhancement images show no evidence of myocardial scar. *LA* = left atrium, *LV* = left ventricle.

perfusion imaging with a comprehensive assessment of biventricular function, regional function (wall thickening or strain imaging), and edema and infarction imaging, all at high spatial resolution and tissue contrast. Recently Coelho-Filho (79) and colleagues demonstrated that stress myocardial perfusion cardiac MR may be an effective alternative to achieving sex equality in diagnosing CAD and in risk stratification for cardiovascular imaging. In a relatively large cohort of women and men, there were no significant sex differences for diagnosing CAD or for risk stratification of major adverse cardiovascular events by using stress myocardial perfusion cardiac MR imaging. A recently published expert consensus document on cardiac MR imaging (80) ranked stress myocardial perfusion cardiac MR as a primary form of testing for *(a)* identifying patients with ischemic heart disease when there are resting electrocardiographic abnormalities or they have inability to exercise, *(b)* identifying patients with large-vessel CAD and its distribution who are candidates for interventional procedures, or *(c)* identifying patients who are appropriate candidates for interventional procedures. This suggests that stress myocardial perfusion cardiac MR is more than an effective alternative for diagnosing CAD and is increasingly viewed as a powerful cardiac prognostication tool in patients with chest pain patients and those suspected of having CAD (81–83).

Special Populations

Myocardial perfusion cardiac MR is ideally suited to resolve imaging challenges posed by particular patient populations. In women, breast attenuation artifacts, smaller-sized hearts, and limited exercise tolerance may limit noninvasive CAD detection (84–86). Stress myocardial perfusion cardiac MR provides high-resolution images for assessment of myocardial ischemia at high tissue contrast without exposing patients to radiation. Klem et al (73) found excellent sensitivity and specificity (0.84 and 0.88, respectively) in women, confirming the usefulness of stress myocardial

CI: 0.78, 0.83) for detection of CAD. Adenosine stress testing had better sensitivity for diagnosing CAD than did dipyridamole (0.90; 95% CI: 0.88, 0.92 vs 0.86, 95% CI: 0.80, 0.90; *P* = .022) and a tendency to a better specificity (0.81, 95% CI: 0.78, 0.84 vs 0.77, 95% CI: 0.71, 0.82; *P* = .065). Table 2 presents the diagnostic performance of stress myocardial perfusion cardiac MR imaging in selected studies. Stress

myocardial perfusion data also correlate strongly with invasive coronary blood flow measurement by fractional flow reserve, reinforcing its clinical application in the diagnosis and treatment planning of CAD.

Compared with nuclear techniques and the recently developed stress multidetector computed tomography (CT), stress myocardial perfusion cardiac MR imaging allows integration of myocardial

Radiology

Table 2

Characteristics of a Selective List of Studies of the Diagnostic Performance of Stress Myocardial Perfusion MR Imaging

Author and Year*	No. of Patients	Criterion for Significant CAD	Stress Agent	Sensitivity	Specificity
Schwitter et al, 2001 (48)	48	Stenosis ≥ 50%	Dipyridamole	0.86	0.80
Doyle et al, 2003 (55)	229	Stenosis ≥ 70%	Dipyridamole	0.58	0.78
Ishida et al, 2003 (56)	104	Stenosis > 70%	Dipyridamole	0.90	0.85
Nagel et al, 2003 (57)	90	Stenosis ≥ 75%	Adenosine	0.88	0.90
Giang et al, 2004 (51)	94	Stenosis ≥ 50%	Adenosine	0.87	0.86
Kawase et al, 2004 (58)	50	Stenosis > 70%	Nicorandil	0.94	0.94
Paetsch et al, 2004 (59)	79	Stenosis > 50%	Adenosine	0.91	0.62
Plein et al, 2004 (60)	72	Stenosis ≥ 70%	Adenosine	0.88	0.83
Takase et al, 2004 (61)	102	Stenosis > 50%	Dipyridamole	0.93	0.85
Thiele et al, 2004 (62)	20	Stenosis ≥ 70%	Adenosine	0.75	0.58
Plein et al, 2005 (63)	92	Stenosis > 70%	Adenosine	0.88	0.74
Sakuma et al, 2005 (64)	40	Stenosis > 70%	Dipyridamole	0.81	0.68
Cury et al, 2006 (65)	47	Stenosis ≥ 70%	Dipyridamole	0.93	0.64
Klem et al, 2006 (30)	100	Stenosis ≥ 70%	Adenosine	0.84	0.58
Pilz et al, 2006 (66)	176	Stenosis > 70%	Adenosine	0.96	0.83
Merkle et al, 2007 (67)	228	Stenosis > 70%	Adenosine	0.96	0.72
Cheng et al, 2007 (29)	65	Stenosis ≥ 50%	Adenosine	0.90	0.67
Greenwood et al, 2007 (68)	35	Stenosis ≥ 70%	Adenosine	0.72	1.0
Seeger et al, 2007 (69)	51	Stenosis > 70%	Adenosine	0.92	0.85
Gebker et al, 2008 (37)	101	Stenosis ≥ 50%	Adenosine	0.90	0.71
Meyer et al, 2008 (70)	60	Stenosis > 70%	Adenosine	0.89	0.79
Pilz et al, 2008 (71)	22	Stenosis > 70%	Adenosine	0.92	1.0
Schwitter et al, 2008 (52)	225	Stenosis ≥ 50%	Adenosine	0.85	0.67
Klein et al, 2008 (72)	54	Stenosis ≥ 50%	Adenosine	0.87	0.88
Klem et al, 2008 (73)	147	Stenosis ≥ 70%	Adenosine	0.84	0.88
Thomas et al, 2008 (74)	60	Stenosis ≥ 50%	Adenosine	0.93	0.84
Burgstahler et al, 2008 (75)	23	Stenosis ≥ 70%	Adenosine	1.0	0.80
Arnold et al, 2010 (76)	65	Stenosis ≥ 50%	Adenosine	0.90	0.81
Manka et al, 2010 (77)	41	Stenosis ≥ 50%	Adenosine	0.92	0.75
Lockie et al, 2011 (78)	42	Fractional flow reserve < 0.75	Adenosine	0.82	0.94

* Numbers in parentheses are reference numbers.

perfusion cardiac MR in this challenging population. Myocardial perfusion cardiac MR also provides insight into the physiopathology of chest pain with normal epicardial coronary arteries, a vexing clinical problem commonly present in women. Panting et al (87) identified subendocardial myocardial hypoperfusion during adenosine infusion in mostly female patients with chest pain and no epicardial coronary stenosis (syndrome X), and Doyle et al (55) reported a reduced transmural perfusion reserve in a similar class of patients. A reduced myocardial or coronary flow reserve was also reported in hypertension and myocardial hypertrophy (88,89) and with some cardiomyopathies (90). Therefore, myocardial stress

perfusion cardiac MR helps identify an abnormal coronary microcirculation to explain the symptoms, even if the precise mechanism cannot be elucidated. Possible explanations range from impaired smooth muscle function to a reduced capillary density and endothelial dysfunction.

Myocardial Perfusion Imaging for Prognosis in CAD

Growing evidence indicates that myocardial perfusion cardiac MR can provide strong prognostic information about cardiac events in various clinical scenarios, which has supported its more widespread use in patient care. Ingkanison et al (81) demonstrated

that an adenosine perfusion cardiac MR study can determine prognosis in patients presenting with chest pain, a nondiagnostic electrocardiogram, and negative serum biomarkers for myocardial infarction. In such patients, a negative stress perfusion cardiac MR examination was associated with an excellent negative predictive value for subsequent diagnosis of CAD or an adverse clinical outcome. No patient with a normal stress perfusion cardiac MR examination experienced a major adverse cardiac event during follow-up. In a cohort of 513 patients suspected of having myocardial ischemia, Jahnke et al (91) examined the value of stress myocardial perfusion cardiac MR to help predict cardiac death and nonfatal myocardial

infarction. At 3 years, the event-free survival was 99.2% for patients with normal perfusion cardiac MR examination and 83.5% for those with abnormal perfusion examination. An abnormal myocardial perfusion cardiac MR examination was associated with an increased likelihood of death or nonfatal infarction over the risk estimated from clinical risk factors (likelihood ratio, χ^2 = 16.0–34.3, $P < .001$), clearly identifying patients at risk for future cardiac events. Our group has also demonstrated that stress myocardial perfusion cardiac MR provides complementary prognostic data beyond clinical factors and scar imaging at late gadolinium enhancement (83). In a consecutive cohort of patients referred for myocardial ischemia assessment with stress cardiac MR, an abnormal myocardial perfusion cardiac examination maintained a more than three-fold adjusted association with cardiac death or acute myocardial infarction. Further information regarding the optimal integration of stress perfusion cardiac MR in existing diagnostic strategies and how its prognostic information can be best utilized is expected from the upcoming IMPACT II and CE-MARC studies (91).

Novel Clinical Applications for Myocardial Perfusion Assessment

The assessment of myocardial blood flow with stress myocardial perfusion cardiac MR has the potential to detect structural and physiologic abnormalities beyond epicardial coronary disease such as adverse microvascular remodeling and coronary microvascular dysfunction. In patients with hypertrophic cardiomyopathy, reduced myocardial perfusion reserve particularly in the endocardium, as measured with stress myocardial perfusion cardiac MR imaging, has been shown to be present and to be associated with the magnitude of wall thickness and hypertrophy (92). While the severity of hypertrophy has been associated with the risk of sudden death, the underlining pathophysiological mechanism remains unclear. However, the association between impaired myocardial blood flow reserve and the

magnitude of the hypertrophy suggest that coronary microvascular dysfunction may be involved in the increased risk of sudden death. Abnormal resting blood flow has also been reported in patients with idiopathic dilated cardiomyopathy who were found to have increased extracellular matrix remodeling as assessed with quantification of blood-tissue partition coefficient for the extracellular contrast (93). Recently Cook et al (94) demonstrated that a significant impairment in transmural perfusion reserve ratio is present in patients with aortic coarctation, both with and without any residual stenosis.

Cardiac MR perfusion imaging may potentially also play a role in depicting early adverse changes in the microcirculation as a result of cardiovascular risk factors. As part of the Multi-Ethnic Study of Atherosclerosis, it was shown that hyperemic myocardial blood flow response was attenuated in asymptomatic individuals with a greater coronary risk factor burden, in particular hypertension, and elevated blood lipid levels (95). In patients with diabetes and autonomic neuropathy, the vasodilator response was found to be significantly lower than that in patients with diabetes but without neuropathy (96). This and at least one other study (97) have suggested a link between sympathetic innervation of the heart and the coronary vasodilator response, when other traditional measures of cardiac function were within the normal range, and in the absence of any signs or symptoms of coronary disease.

Cardiac MR Perfusion in Pediatric Patients and Congenital Heart Disease

Though cardiac MR imaging in pediatric patients has become routine at many heart centers, its practice only seldom includes myocardial perfusion studies. The awareness about the indications for myocardial perfusion cardiac MR in pediatric patients may be lower than for CAD (98). Also, safety and cost concerns may hamper referrals of pediatric patients for MR studies, since sedation is required in very young children and infants (99). The

safety of pharmacologic vasodilation has been extensively studied in adults with CAD, but the uniqueness and complexity of congenital heart defects may have led to additional reluctance to perform similar tests in pediatric patients.

Two potential applications of cardiac MR myocardial perfusion imaging in pediatric patients are (a) clinical indications for the detection of ischemia before medical therapy or revascularization and (b) detection of microvascular dysfunction in various congenital heart diseases. For the former, Figure 5 is an example from a 13-year-old female patient who presented with syncope, elevation of heart enzymes, and ST elevation in the left-sided precordial leads at exercise stress testing but only mild symptoms of angina pectoris. Cardiac MR with 3D reconstruction of the anatomy revealed a left coronary artery arising from the right coronary artery with an aberrant course between the main pulmonary artery and the aortic root (Fig 4a). Cardiac MR myocardial perfusion showed severe anterolateral ischemia (Fig 4b), with quantified stress perfusion of 1.4 mL/g/min in that region as opposed to 2.1 mL/g/min in the remote area and normal perfusion at rest. Viability and wall motion analysis at rest were normal. Heart catheterization confirmed the suspicion of a dynamic stenosis. Therefore, minimal invasive direct coronary artery bypass surgery was performed consecutively, resulting in normalized stress perfusion cardiac MR examination at follow-up 3 months later.

Other examples of first-pass cardiac MR perfusion imaging in children with clinical consequences have been reported for the Bland-White-Garland syndrome (or anomalous left coronary artery originating from the pulmonary artery [ALCAPA] syndrome), Kawaski disease, coronary fistulas, and in patients with transposition of the great arteries after arterial switch operation (100). In the latter group, corrective surgery includes transfer of the coronary arteries. Coronary problems have been identified as a risk factor for acute and long-term sequelae (101,102).

The second group of possible indications for cardiac MR perfusion

Figure 5

a. b.
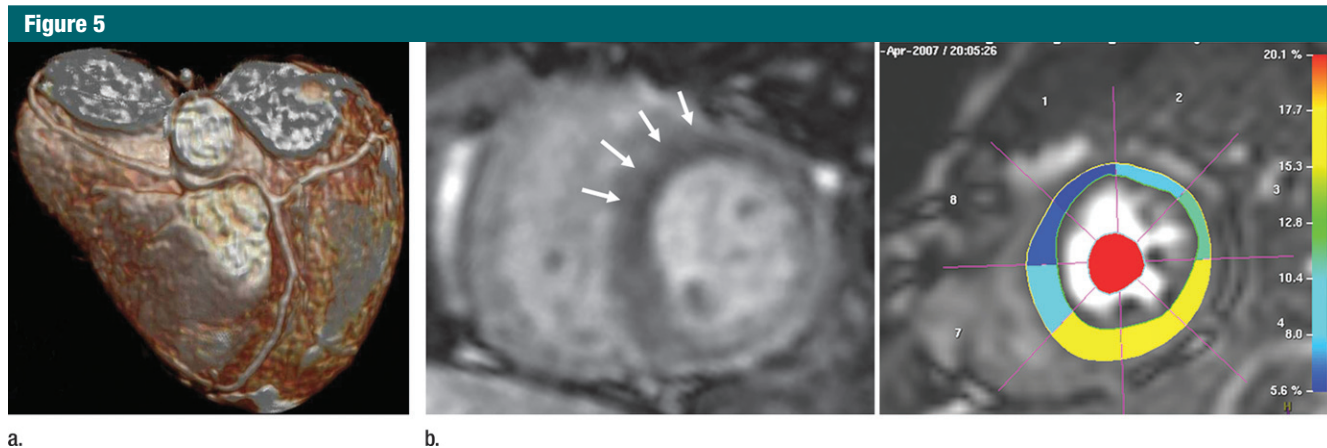
Figure 5: **(a)** A 3D reconstruction of whole-heart MR angiography data set shows that left coronary artery arises from right coronary artery with a course between main pulmonary artery and aortic root, resulting in a dynamic stenosis. **(b)** Left: Preoperative stress perfusion MR image (medium dose of adenosine, 100 µg/kg/min) shows severe ischemia in anterolateral left-ventricular wall (arrows). Right: Color-coded illustration of perfusion distribution derived from the up-slope (arbitrary units of signal intensity/time increment between images) of the regional signal intensity curves depicts the rate of contrast enhancement in eight segments.

studies in pediatric patients, the detection of microvascular dysfunction, is not yet established clinically, though the clinical implications for an individual patient or a patient group are increasingly appreciated (103). Findings of studies on hypertrophic cardiomyopathy in childhood have shown that individuals with early onset of the disease, in particular, develop wall hypertrophy, a known independent risk factor for sudden cardiac death in hypertrophic cardiomyopathy (103–106). Myocardial perfusion imaging in conjunction with cine MR imaging for the assessment of left ventricular wall thickness may be able to identify patients at risk (107).

We performed first-pass perfusion in patients with transposition of the great arteries after arterial switch operation (108) and in patients with hypoplastic left heart syndrome. Myocardial blood flow quantification showed a reduced global perfusion reserve in both patient groups, in accordance with a study by Hauser et al, who applied PET perfusion imaging to patients with transposition of the great arteries (109). Other interesting and important potential indications for a perfusion cardiac MR in children are metabolic diseases, such as diabetes mellitus, evaluation for signs of heart transplant rejection, and various conditions with pressure- or volume- overloaded left or right

ventricles (eg, tetralogy of Fallot, aortic stenosis). Recently, Vogel-Claussen et al (110), utilizing cardiac MR, showed a significantly reduced right and left ventricular perfusion reserve in patients with pulmonary hypertension. The authors found that biventricular perfusion reserve inversely correlates with right ventricular workload and ejection fraction. Van Wolferen and colleagues (111) used MR imaging phase-contrast measurements to show that right coronary artery flow, but not left coronary artery flow, had a significantly smaller systolic-to-diastolic flow ratio compared with that in healthy control subjects. The systolic-to-diastolic flow ratio in the right coronary artery correlated inversely with the right ventricular pressure. In an experimental model of chronic right ventricular hypertrophy in swine, we were able to demonstrate a reduced myocardial perfusion reserve prior to right ventricular failure (112). Perfusion cardiac MR may help to improve our understanding of the underlying pathophysiology of the microvascular bed in congenital heart disease, which is arguably a prerequisite for developing new treatments.

Limitations

The commonly used gadolinium-based cardiac MR contrast agents currently do

not have regulatory approval for any cardiac indication in the United States. This means that gadolinium-based agents are used off-label for cardiac perfusion imaging. Similarly, vendors of MR equipment are not allowed to market cardiac perfusion imaging techniques in the United States. Furthermore, the application of cardiac MR for ischemia detection during vasodilator stress would require pursuing two unapproved indications, and this regulatory hurdle has proved difficult to overcome.

The administration of vasodilator stress agents (eg, adenosine) in the MR imaging environment is considered more challenging than when other imaging modalities (eg, PET or SPECT) are used. A new vasodilator stress agent, regadenoson (113) (now approved by the Food and Drug Administration), has reduced symptom intensity and gives greater patient tolerance. It is delivered as a single bolus, which allows administration outside the magnet.

The number of centers currently performing cardiac MR perfusion imaging is arguably still limited by a lack of training opportunities in this area, and cardiac MR in general. The logistical hurdles for perfusion cardiac MR are related to operating in an environment with strong magnetic fields, requiring radiofrequency shielding of the imager, and limiting imaging of patients with certain types of

devices (eg, pacemakers and implantable cardiac defibrillators) that are generally unsuitable for this type of environment. Nevertheless, cardiac device manufacturers see sufficient potential in cardiac MR to have brought to market cardiac MR–compatible pacemakers and similar efforts are underway for implantable cardiac defibrillators. A new generation of short-bore 1.5- and 3-T magnets has removed most hurdles for placing such imagers into the cardiovascular imaging and/or catheterization laboratories. It can be argued that the logistics of cardiac MR perfusion imaging are no more ornery than those of nuclear imaging, with the important difference that in the latter case economies of scale and several decades of experience and trials have led to general acceptance of the logistical requirements. In several countries, reimbursement for cardiac MR studies, in general, and cardiac MR perfusion studies continues to be a barrier for wider clinical use. Furthermore, more efforts need be expanded to educate referring physicians and patients about the benefits of clinical cardiac MR imaging.

In conclusion, a comprehensive cardiac MR study provides high accurate assessment of myocardial physiology, including myocardial perfusion, assessment of CAD, myocardial infarction, and ventricular function. Growing evidence from clinical and prognostic studies strongly supports the application of myocardial perfusion imaging with cardiac MR as a diagnostic and prognostic tool to guide medical therapy in the clinical setting. During the past decade, the myocardial perfusion assessment with cardiac MR has evolved into a powerful clinical tool, which helps clinicians diagnose and better understand several important cardiac conditions.

References

1. Klocke FJ. Measurements of coronary flow reserve: defining pathophysiology versus making decisions about patient care. Circulation 1987;76(6):1183–1189.

2. Kjaer A, Meyer C, Nielsen FS, Parving HH, Hesse B. Dipyridamole, cold pressor test, and demonstration of endothelial dysfunction: a PET study of myocardial perfusion in diabetes. J Nucl Med 2003;44(1):19–23.

3. Gould KL, Kirkeeide RL, Buchi M. Coronary flow reserve as a physiologic measure of stenosis severity. J Am Coll Cardiol 1990;15(2):459–474.

4. Gould KL, Lipscomb K. Effects of coronary stenoses on coronary flow reserve and resistance. Am J Cardiol 1974;34(1):48–55.

5. Duncker DJ, Bache RJ. Regulation of coronary blood flow during exercise. Physiol Rev 2008;88(3):1009–1086.

6. Geldof MJ, Schalij MJ, Manger Cats V, et al. Comparison between regional myocardial perfusion reserve and coronary flow reserve in the canine heart. Eur Heart J 1995;16(12):1860–1871.

7. Serruys PW, di Mario C, Piek J, et al. Prognostic value of intracoronary flow velocity and diameter stenosis in assessing the short- and long-term outcomes of coronary balloon angioplasty: the DEBATE Study (Doppler Endpoints Balloon Angioplasty Trial Europe). Circulation 1997;96(10):3369–3377.

8. Nagel E, Thouet T, Klein C, et al. Noninvasive determination of coronary blood flow velocity with cardiovascular magnetic resonance in patients after stent deployment. Circulation 2003;107(13):1738–1743.

9. Detre JA, Zhang W, Roberts DA, et al. Tissue specific perfusion imaging using arterial spin labeling. NMR Biomed 1994;7(1-2):75–82.

10. Vandsburger MH, Janiczek RL, Xu Y, et al. Improved arterial spin labeling after myocardial infarction in mice using cardiac and respiratory gated look-locker imaging with fuzzy C-means clustering. Magn Reson Med 2010;63(3):648–657.

11. Wang J, Licht DJ, Silvestre DW, Detre JA. Why perfusion in neonates with congenital heart defects is negative: technical issues related to pulsed arterial spin labeling. Magn Reson Imaging 2006;24(3):249–254.

12. Tsekos NV, Zhang Y, Merkle H, et al. Fast anatomical imaging of the heart and assessment of myocardial perfusion with arrhythmia insensitive magnetization preparation. Magn Reson Med 1995;34(4):530–536.

13. Panting JR, Gatehouse PD, Yang GZ, et al. Echo-planar magnetic resonance myocardial perfusion imaging: parametric map analysis and comparison with thallium SPECT. J Magn Reson Imaging 2001;13(2):192–200.

14. Ding S, Wolff SD, Epstein FH. Improved coverage in dynamic contrast-enhanced cardiac MRI using interleaved gradient-echo EPI. Magn Reson Med 1998;39(4):514–519.

15. Wieben O, Francois C, Reeder SB. Cardiac MRI of ischemic heart disease at 3 T: potential and challenges. Eur J Radiol 2008;65(1):15–28.

16. Ferreira P, Gatehouse P, Bucciarelli-Ducci C, Wage R, Firmin D. Measurement of myocardial frequency offsets during first pass of a gadolinium-based contrast agent in perfusion studies. Magn Reson Med 2008;60(4):860–870.

17. Christian TF, Aletras AH, Arai AE. Estimation of absolute myocardial blood flow during first-pass MR perfusion imaging using a dual-bolus injection technique: comparison to single-bolus injection method. J Magn Reson Imaging 2008;27(6):1271–1277.

18. Gatehouse PD, Elkington AG, Ablitt NA, Yang GZ, Pennell DJ, Firmin DN. Accurate assessment of the arterial input function during high-dose myocardial perfusion cardiovascular magnetic resonance. J Magn Reson Imaging 2004;20(1):39–45.

19. Cleppien DE, Horstick G, Abegunewardene N, et al. Comparison of the quantitative first pass myocardial perfusion MRI with and without prospective slice tracking: comparison between breath-hold and free-breathing condition. Magn Reson Med 2010;64(5):1461–1470.

20. Pedersen H, Kelle S, Ringgaard S, et al. Quantification of myocardial perfusion using free-breathing MRI and prospective slice tracking. Magn Reson Med 2009;61(3):734–738.

21. Milles J, van der Geest RJ, Jerosch-Herold M, Reiber JH, Lelieveldt BP. Fully automated motion correction in first-pass myocardial perfusion MR image sequences. IEEE Trans Med Imaging 2008;27(11):1611–1621.

22. Niendorf T, Sodickson DK. Parallel imaging in cardiovascular MRI: methods and applications. NMR Biomed 2006;19(3):325–341.

23. Oesterle C, Strohschein R, Köhler M, Schnell M, Hennig J. Benefits and pitfalls of keyhole imaging, especially in first-pass perfusion studies. J Magn Reson Imaging 2000;11(3):312–323.

24. Gebker R, Jahnke C, Paetsch I, et al. MR myocardial perfusion imaging with k-space and time broad-use linear acquisition speed-up technique: feasibility study. Radiology 2007;245(3):863–871.

25. Plein S, Ryf S, Schwitter J, Radjenovic A, Boesiger P, Kozerke S. Dynamic contrast-enhanced myocardial perfusion MRI accelerated with k-t sense. Magn Reson Med 2007; 58(4):777–785.

26. Vijayakumar S, Huang F, R Dibella E. Improved partial k-space reconstruction technique for dynamic myocardial perfusion MRI. Conf Proc IEEE Eng Med Biol Soc 2005; 2:1419–1421.

27. Huang F, Akao J, Vijayakumar S, Duensing GR, Limkeman M. k-t GRAPPA: a k-space implementation for dynamic MRI with high reduction factor. Magn Reson Med 2005; 54(5):1172–1184.

28. Jung B, Honal M, Hennig J, Markl M. k-t-Space accelerated myocardial perfusion. J Magn Reson Imaging 2008;28(5):1080–1085.

29. Cheng AS, Pegg TJ, Karamitsos TD, et al. Cardiovascular magnetic resonance perfusion imaging at 3-tesla for the detection of coronary artery disease: a comparison with 1.5-tesla. J Am Coll Cardiol 2007; 49(25):2440–2449.

30. Klem I, Heitner JF, Shah DJ, et al. Improved detection of coronary artery disease by stress perfusion cardiovascular magnetic resonance with the use of delayed enhancement infarction imaging. J Am Coll Cardiol 2006;47(8):1630–1638.

31. Vitanis V, Manka R, Boesiger P, Kozerke S. High resolution 3D cardiac perfusion imaging using compartment-based k-t PCA. Conf Proc IEEE Eng Med Biol Soc 2010;2010: 21–24.

32. Candes EJ, Wakin MB. An introduction to compressive sampling. IEEE Signal Process Mag 2008;25(2):21–30.

33. Lustig M, Donoho D, Pauly JM. Sparse MRI: the application of compressed sensing for rapid MR imaging. Magn Reson Med 2007;58(6):1182–1195.

34. Otazo R, Kim D, Axel L, Sodickson DK. Combination of compressed sensing and parallel imaging for highly accelerated first-pass cardiac perfusion MRI. Magn Reson Med 2010;64(3):767–776.

35. Mistretta CA. Undersampled radial MR acquisition and highly constrained back projection (HYPR) reconstruction: potential medical imaging applications in the post-Nyquist era. J Magn Reson Imaging 2009; 29(3):501–516.

36. Ge L, Kino A, Lee D, Dharmakumar R, Carr JC, Li D. Myocardial perfusion magnetic resonance imaging using sliding-window conjugate-gradient HYPR methods in canine with stenotic coronary arteries.

J Comput Assist Tomogr 2010;34(5):684–688.

37. Gebker R, Jahnke C, Paetsch I, et al. Diagnostic performance of myocardial perfusion MR at 3 T in patients with coronary artery disease. Radiology 2008;247(1):57–63.

38. Kraitchman DL, Chin BB, Heldman AW, Solaiyappan M, Bluemke DA. MRI detection of myocardial perfusion defects due to coronary artery stenosis with MS-325. J Magn Reson Imaging 2002;15(2):149–158.

39. Di Bella EV, Parker DL, Sinusas AJ. On the dark rim artifact in dynamic contrast-enhanced MRI myocardial perfusion studies. Magn Reson Med 2005;54(5):1295–1299.

40. Xue H, Zuehlsdorff S, Kellman P, et al. Unsupervised inline analysis of cardiac perfusion MRI. Med Image Comput Comput Assist Interv 2009;12(Pt 2):741–749.

41. Ruan C, Yang S, Clarke GD, et al. First-pass contrast-enhanced myocardial perfusion MRI using a maximum up-slope parametric map. IEEE Trans Inf Technol Biomed 2006;10(3):574–580.

42. Penzkofer H, Wintersperger BJ, Knez A, Weber J, Reiser M. Assessment of myocardial perfusion using multisection first-pass MRI and color-coded parameter maps: a comparison to 99mTc Sesta MIBI SPECT and systolic myocardial wall thickening analysis. Magn Reson Imaging 1999; 17(2):161–170.

43. Jerosch-Herold M, Swingen C, Seethamraju RT. Myocardial blood flow quantification with MRI by model-independent deconvolution. Med Phys 2002;29(5):886–897.

44. Jerosch-Herold M, Hu XD, Murthy NS, Rickers C, Stillman AE. Magnetic resonance imaging of myocardial contrast enhancement with MS-325 and its relation to myocardial blood flow and the perfusion reserve. J Magn Reson Imaging 2003;18(5):544–554.

45. Futamatsu H, Wilke N, Klassen C, et al. Evaluation of cardiac magnetic resonance imaging parameters to detect anatomically and hemodynamically significant coronary artery disease. Am Heart J 2007; 154(2):298–305.

46. Neyran B, Janier MF, Casali C, Revel D, Canet Soulas EP. Mapping myocardial perfusion with an intravascular MR contrast agent: robustness of deconvolution methods at various blood flows. Magn Reson Med 2002;48(1):166–179.

47. Wilke N, Simm C, Zhang J, et al. Contrast-enhanced first pass myocardial perfusion imaging: correlation between myocardial blood flow in dogs at rest and

during hyperemia. Magn Reson Med 1993; 29(4):485–497.

48. Schwitter J, Nanz D, Kneifel S, et al. Assessment of myocardial perfusion in coronary artery disease by magnetic resonance: a comparison with positron emission tomography and coronary angiography. Circulation 2001;103(18):2230–2235.

49. Al-Saadi N, Nagel E, Gross M, et al. Noninvasive detection of myocardial ischemia from perfusion reserve based on cardiovascular magnetic resonance. Circulation 2000; 101(12):1379–1383.

50. Wolff SD, Schwitter J, Coulden R, et al. Myocardial first-pass perfusion magnetic resonance imaging: a multicenter dose-ranging study. Circulation 2004;110(6): 732–737.

51. Giang TH, Nanz D, Coulden R, et al. Detection of coronary artery disease by magnetic resonance myocardial perfusion imaging with various contrast medium doses: first European multi-centre experience. Eur Heart J 2004;25(18):1657–1665.

52. Schwitter J, Wacker CM, van Rossum AC, et al. MR-IMPACT: comparison of perfusion-cardiac magnetic resonance with single-photon emission computed tomography for the detection of coronary artery disease in a multicentre, multivendor, randomized trial. Eur Heart J 2008;29(4):480–489.

53. Nandalur KR, Dwamena BA, Choudhri AF, Nandalur MR, Carlos RC. Diagnostic performance of stress cardiac magnetic resonance imaging in the detection of coronary artery disease: a meta-analysis. J Am Coll Cardiol 2007;50(14):1343–1353.

54. Hamon M, Fau G, Née G, Ehtisham J, Morello R, Hamon M. Meta-analysis of the diagnostic performance of stress perfusion cardiovascular magnetic resonance for detection of coronary artery disease. J Cardiovasc Magn Reson 2010;12(1):29.

55. Doyle M, Fuisz A, Kortright E, et al. The impact of myocardial flow reserve on the detection of coronary artery disease by perfusion imaging methods: an NHLBI WISE study. J Cardiovasc Magn Reson 2003; 5(3):475–485.

56. Ishida N, Sakuma H, Motoyasu M, et al. Noninfarcted myocardium: correlation between dynamic first-pass contrast-enhanced myocardial MR imaging and quantitative coronary angiography. Radiology 2003;229(1):209–216.

57. Nagel E, Klein C, Paetsch I, et al. Magnetic resonance perfusion measurements for the noninvasive detection of coronary artery disease. Circulation 2003;108(4):432–437.

58. Kawase Y, Nishimoto M, Hato K, Okajima K, Yoshikawa J. Assessment of coronary artery disease with nicorandil stress magnetic resonance imaging. Osaka City Med J 2004;50(2):87–94.

59. Paetsch I, Jahnke C, Wahl A, et al. Comparison of dobutamine stress magnetic resonance, adenosine stress magnetic resonance, and adenosine stress magnetic resonance perfusion. Circulation 2004;110(7):835–842.

60. Plein S, Greenwood JP, Ridgway JP, Cranny G, Ball SG, Sivananthan MU. Assessment of non-ST-segment elevation acute coronary syndromes with cardiac magnetic resonance imaging. J Am Coll Cardiol 2004;44(11):2173–2181.

61. Takase B, Nagata M, Kihara T, et al. Whole-heart dipyridamole stress first-pass myocardial perfusion MRI for the detection of coronary artery disease. Jpn Heart J 2004;45(3):475–486.

62. Thiele H, Plein S, Breeuwer M, et al. Color-encoded semiautomatic analysis of multi-slice first-pass magnetic resonance perfusion: comparison to tetrofosmin single photon emission computed tomography perfusion and X-ray angiography. Int J Cardiovasc Imaging 2004;20(5):371–384; discussion 385–387.

63. Plein S, Radjenovic A, Ridgway JP, et al. Coronary artery disease: myocardial perfusion MR imaging with sensitivity encoding versus conventional angiography. Radiology 2005;235(2):423–430.

64. Sakuma H, Suzawa N, Ichikawa Y, et al. Diagnostic accuracy of stress first-pass contrast-enhanced myocardial perfusion MRI compared with stress myocardial perfusion scintigraphy. AJR Am J Roentgenol 2005;185(1):95–102.

65. Cury RC, Cattani CA, Gabure LA, et al. Diagnostic performance of stress perfusion and delayed-enhancement MR imaging in patients with coronary artery disease. Radiology 2006;240(1):39–45.

66. Pilz G, Bernhardt P, Klos M, Ali E, Wild M, Höfling B. Clinical implication of adenosine-stress cardiac magnetic resonance imaging as potential gatekeeper prior to invasive examination in patients with AHA/ACC class II indication for coronary angiography. Clin Res Cardiol 2006;95(10):531–538.

67. Merkle N, Wöhrle J, Grebe O, et al. Assessment of myocardial perfusion for detection of coronary artery stenoses by steady-state, free-precession magnetic resonance first-pass imaging. Heart 2007;93(11):1381–1385.

68. Greenwood JP, Younger JF, Ridgway JP, Sivananthan MU, Ball SG, Plein S. Safety and diagnostic accuracy of stress cardiac magnetic resonance imaging vs exercise tolerance testing early after acute ST elevation myocardial infarction. Heart 2007;93(11):1363–1368.

69. Seeger A, Doesch C, Klumpp B, et al. MR stress perfusion for the detection of flow-limiting stenoses in symptomatic patients with known coronary artery disease and history of stent implantation [in German]. Rofo 2007;179(10):1068–1073.

70. Meyer C, Strach K, Thomas D, et al. High-resolution myocardial stress perfusion at 3 T in patients with suspected coronary artery disease. Eur Radiol 2008;18(2):226–233.

71. Pilz G, Klos M, Ali E, Hoefling B, Scheck R, Bernhardt P. Angiographic correlations of patients with small vessel disease diagnosed by adenosine-stress cardiac magnetic resonance imaging. J Cardiovasc Magn Reson 2008;10:8.

72. Klein C, Gebker R, Kokocinski T, et al. Combined magnetic resonance coronary artery imaging, myocardial perfusion and late gadolinium enhancement in patients with suspected coronary artery disease. J Cardiovasc Magn Reson 2008;10:45.

73. Klem I, Greulich S, Heitner JF, et al. Value of cardiovascular magnetic resonance stress perfusion testing for the detection of coronary artery disease in women. JACC Cardiovasc Imaging 2008;1(4):436–445.

74. Thomas D, Strach K, Meyer C, et al. Combined myocardial stress perfusion imaging and myocardial stress tagging for detection of coronary artery disease at 3 Tesla. J Cardiovasc Magn Reson 2008;10:59.

75. Burgstahler C, Kunze M, Gawaz MP, et al. Adenosine stress first pass perfusion for the detection of coronary artery disease in patients with aortic stenosis: a feasibility study. Int J Cardiovasc Imaging 2008;24(2):195–200.

76. Arnold JR, Karamitsos TD, Pegg TJ, et al. Adenosine stress myocardial contrast echocardiography for the detection of coronary artery disease: a comparison with coronary angiography and cardiac magnetic resonance. JACC Cardiovasc Imaging 2010;3(9):934–943.

77. Manka R, Jahnke C, Gebker R, Schnackenburg B, Paetsch I. Head-to-head comparison of first-pass MR perfusion imaging during adenosine and high-dose dobutamine/atropine stress. Int J Cardiovasc Imaging 2011; 27(7):995–1002.

78. Lockie T, Ishida M, Perera D, et al. High-resolution magnetic resonance myocardial perfusion imaging at 3.0-Tesla to detect hemodynamically significant coronary stenoses as determined by fractional flow reserve. J Am Coll Cardiol 2011;57(1):70–75.

79. Coelho-Filho OR, Seabra LF, Mongeon FP, et al. Stress myocardial perfusion imaging by CMR provides strong prognostic value to cardiac events regardless of patient's sex. JACC Cardiovasc Imaging 2011;4(8):850–861.

80. American College of Cardiology Foundation Task Force on Expert Consensus Documents, Hundley WG, Bluemke DA, et al. ACCF/ACR/AHA/NASCI/SCMR 2010 expert consensus document on cardiovascular magnetic resonance: a report of the American College of Cardiology Foundation Task Force on Expert Consensus Documents. Circulation 2010;121(22):2462–2508.

81. Ingkanisorn WP, Kwong RY, Bohme NS, et al. Prognosis of negative adenosine stress magnetic resonance in patients presenting to an emergency department with chest pain. J Am Coll Cardiol 2006;47(7):1427–1432.

82. Kwong RY, Schussheim AE, Rekhraj S, et al. Detecting acute coronary syndrome in the emergency department with cardiac magnetic resonance imaging. Circulation 2003;107(4):531–537.

83. Steel K, Broderick R, Gandla V, et al. Complementary prognostic values of stress myocardial perfusion and late gadolinium enhancement imaging by cardiac magnetic resonance in patients with known or suspected coronary artery disease. Circulation 2009;120(14):1390–1400.

84. Kwok Y, Kim C, Grady D, Segal M, Redberg R. Meta-analysis of exercise testing to detect coronary artery disease in women. Am J Cardiol 1999;83(5):660–666.

85. Mieres JH, Shaw LJ, Arai A, et al. Role of noninvasive testing in the clinical evaluation of women with suspected coronary artery disease: Consensus statement from the Cardiac Imaging Committee, Council on Clinical Cardiology, and the Cardiovascular Imaging and Intervention Committee, Council on Cardiovascular Radiology and Intervention, American Heart Association. Circulation 2005;111(5):682–696.

86. Hansen CL, Crabbe D, Rubin S. Lower diagnostic accuracy of thallium-201 SPECT myocardial perfusion imaging in women: an effect of smaller chamber size. J Am Coll Cardiol 1996;28(5):1214–1219.

87. Panting JR, Gatehouse PD, Yang GZ, et al. Abnormal subendocardial perfusion in cardiac syndrome X detected by cardiovascular magnetic resonance imaging. N Engl J Med 2002;346(25):1948–1953.

88. Kelm M, Strauer BE. Coronary flow reserve measurements in hypertension. Med Clin North Am 2004;88(1):99–113.

89. Laine H, Raitakari OT, Niinikoski H, et al. Early impairment of coronary flow reserve in young men with borderline hypertension. J Am Coll Cardiol 1998;32(1):147–153.

90. Weismüller S, Czernin J, Sun KT, Fung C, Phelps ME, Schelbert HR. Coronary vasodilatory capacity is impaired in patients with dilated cardiomyopathy. Am J Card Imaging 1996;10(3):154–162.

91. Jahnke C, Nagel E, Gebker R, et al. Prognostic value of cardiac magnetic resonance stress tests: adenosine stress perfusion and dobutamine stress wall motion imaging. Circulation 2007;115(13):1769–1776.

92. Petersen SE, Jerosch-Herold M, Hudsmith LE, et al. Evidence for microvascular dysfunction in hypertrophic cardiomyopathy: new insights from multiparametric magnetic resonance imaging. Circulation 2007;115(18):2418–2425.

93. Jerosch-Herold M, Sheridan DC, Kushner JD, et al. Cardiac magnetic resonance imaging of myocardial contrast uptake and blood flow in patients affected with idiopathic or familial dilated cardiomyopathy. Am J Physiol Heart Circ Physiol 2008;295(3):H1234–H1242.

94. Cook SC, Ferketich AK, Raman SV. Myocardial ischemia in asymptomatic adults with repaired aortic coarctation. Int J Cardiol 2009;133(1):95–101.

95. Wang L, Jerosch-Herold M, Jacobs DR, Shahar E, Folsom AR. Coronary risk factors and myocardial perfusion in asymptomatic adults: the Multi-Ethnic Study of Atherosclerosis (MESA). J Am Coll Cardiol 2006;47(3):565–572.

96. Taskiran M, Fritz-Hansen T, Rasmussen V, Larsson HB, Hilsted J. Decreased myocardial perfusion reserve in diabetic autonomic neuropathy. Diabetes 2002;51(11):3306–3310.

97. Di Carli MF, Bianco-Batlles D, Landa ME, et al. Effects of autonomic neuropathy on coronary blood flow in patients with diabetes mellitus. Circulation 1999;100(8):813–819.

98. Prakash A, Powell AJ, Krishnamurthy R, Geva T. Magnetic resonance imaging evaluation of myocardial perfusion and viability in congenital and acquired pediatric heart disease. Am J Cardiol 2004;93(5):657–661.

99. Voges I, Jerosch-Herold M, Plagemann T, et al. Cardiovascular magnetic resonance imaging in childhood - clinical indications and case studies [in German]. Klin Padiatr 2010;222(1):3–12.

100. Manso B, Castellote A, Dos L, Casaldáliga J. Myocardial perfusion magnetic resonance imaging for detecting coronary function anomalies in asymptomatic paediatric patients with a previous arterial switch operation for the transposition of great arteries. Cardiol Young 2010;20(4):410–417.

101. Hutter PA, Bennink GB, Ay L, Raes IB, Hitchcock JF, Meijboom EJ. Influence of coronary anatomy and reimplantation on the long-term outcome of the arterial switch. Eur J Cardiothorac Surg 2000;18(2):207–213.

102. Rickers C, Sasse K, Buchert R, et al. Myocardial viability assessed by positron emission tomography in infants and children after the arterial switch operation and suspected infarction. J Am Coll Cardiol 2000;36(5):1676–1683.

103. Maron BJ. Hypertrophic cardiomyopathy in childhood. Pediatr Clin North Am 2004;51(5):1305–1346.

104. Spirito P, Bellone P, Harris KM, Bernabo P, Bruzzi P, Maron BJ. Magnitude of left ventricular hypertrophy and risk of sudden death in hypertrophic cardiomyopathy. N Engl J Med 2000;342(24):1778–1785.

105. Ostman-Smith I. Hypertrophic cardiomyopathy in childhood and adolescence: strategies to prevent sudden death. Fundam Clin Pharmacol 2010;24(5):637–652.

106. Maron MS, Olivotto I, Maron BJ, et al. The case for myocardial ischemia in hypertrophic cardiomyopathy. J Am Coll Cardiol 2009;54(9):866–875.

107. Rickers C, Wilke NM, Jerosch-Herold M, et al. Utility of cardiac magnetic resonance imaging in the diagnosis of hypertrophic cardiomyopathy. Circulation 2005;112(6):855–861.

108. Rickers C, Jerosch-Herold M, Marienfeld J, et al. Myocardial blood flow and viability in children with transpositon of the great arteries after arterial switch operation assessed with magnetic resonance imaging [abstr]. Circulation 2009;120(18):S611.

109. Hauser M, Bengel FM, Kühn A, et al. Myocardial blood flow and flow reserve after coronary reimplantation in patients after arterial switch and ross operation. Circulation 2001;103(14):1875–1880.

110. Vogel-Claussen J, Skrok J, Shehata ML, et al. Right and left ventricular myocardial perfusion reserves correlate with right ventricular function and pulmonary hemodynamics in patients with pulmonary arterial hypertension. Radiology 2011;258(1):119–127.

111. van Wolferen SA, Marcus JT, Westerhof N, et al. Right coronary artery flow impairment in patients with pulmonary hypertension. Eur Heart J 2008;29(1):120–127.

112. Rickers C, Jerosch-Herold M, Kramer H, et al. Regional myocardial perfusion in an animal model of right ventricular hypertrophy assessed with first pass MRI. In: Abstracts from the Tenth Annual Society for Cardiovascular Magnetic Resonance (SCMR) Scientific Session and the Sixth Meeting of the Euro CMR Working Group. February 2–4, 2007 Rome, Italy. J Cardiovasc Magn Reson 2007;9(2):437–438.

113. Al Jaroudi W, Iskandrian AE. Regadenoson: a new myocardial stress agent. J Am Coll Cardiol 2009;54(13):1123–1130.